Environ. Sci. Technol. **1998**, *32,* 1120−1127

Critical Conditions for CO_2 Hydrate Films To Rest on Submarine CO_2 Pond Surfaces: A Mechanistic Study

RYO OHMURA* AND YASUHIKO H. MORI

Department of Mechanical Engineering, Keio University, 3-14-1 Hiyoshi, Kohoku-ku, Yokohama 223-8522, Japan

The stability of hydrate films formed at the horizontal interface between seawater and denser liquid CO_2 under high pressures (≳35 MPa) is considered to have an insight into the feasibility of the disposal/storage of liquid CO_2 in the deep oceans. Hydrate films formed at the interface (i.e., the surface of a liquid CO_2 pond on the seabed) may be denser than both liquid CO_2 and seawater, may be denser than seawater but lighter than liquid CO_2, or may be lighter than both liquids depending on the ambient pressure (i.e., the depth of the interface) and also on the fractional occupancy of hydrate crystalline cavities by CO_2 molecules. The static force balance between the gravitational forces and the interfacial tension force acting on each hydrate film is formulated, thereby predicting the critical condition beyond which the film may sink into the CO_2 pond or buoy up into the sea, or it may be broken due to an internal stress.

1. Intoduction

This paper is concerned with one of the options of CO_2 disposal or storage presently under investigation in order to evaluate its potential to reduce the CO_2 emissions into the atmosphere and thereby to mitigate the greenhouse effect—the option of the injection of liquefied CO_2 into the oceans deeper than 3000 m where CO_2 is presumed to become denser than seawater because of its higher compressibility (*1*). The CO_2 thus injected at a particular location will be deposited on the sea floor, thereby forming a huge submarine pond (or lake). It is reasonable to assume, based on a thermodynamic phase-equilibrium consideration, that CO_2 hydrate will form at the seawater/liquid CO_2 interface—the presumably flat surface of each CO_2 pond—and grow in the form of a thin planar film, or discrete films, intervening between the two liquid phases (*2*). (There may be an objection to this point, although we do not support it. See Appendix I.) Such hydrate films, if resting on the interface, are expected to retard the CO_2 dissolution from the pond into the adjacent seawater. However, do the hydrate films actually rest on the interface?

Figure 1 compares the mass densities of seawater and liquid CO_2, each varying with the depth in the sea, and the existing literature values of the density of CO_2 hydrate. The rather wide scatter in the hydrate density values is presumably ascribable, though not entirely, to the fact that the CO_2 hydrate is, as a feature distinctive of clathrate hydrates, a nonstoichiometric compound and hence its density can actually vary within a certain range. The density comparison in Figure 1 indicates that the hydrate may be denser than both seawater (saturated with CO_2) and liquid CO_2, intermediate between the two liquids, or less dense than both of them depending on its own crystallographic composition and also on the depth of the interface in the sea. If this is true (as we believe), is it unlikely that some of the hydrate films grown to certain critical dimensions break out of the interface and sink into the pond or, on the contrary, buoy up into the seawater phase, thereby agitating the interfacial region and possibly promoting the CO_2 dissolution? This is an as-yet unanswered question, and it is the very question to be answered in this paper.

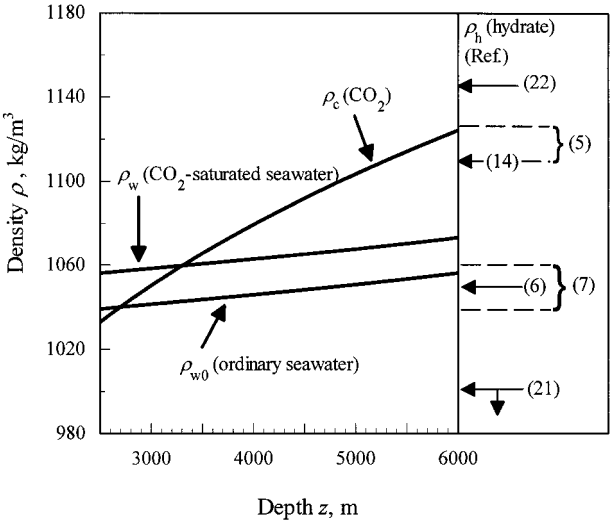

FIGURE 1. Variation with the depth from sea level of the mass densities of normal seawater, CO_2-saturated seawater, and liquid CO_2 in comparison with the values of CO_2 hydrate density reported in the literature. For details, see Appendix I.

This paper includes a mechanistic analysis in which hydrate films are assumed to be rigid planar sheets (section 2), some predictions from the analysis and an assessment based on them (section 3), and a supplementary discussion on possible deflections and resultant breaking of hydrate films assumed to be elastic planar sheets (section 4). Appendices II and III can be used for clarifying how we have evaluated the physical properties of CO_2, ordinary seawater, CO_2-saturated seawater, and the CO_2 hydrate in deducing the numerical predictions shown in section 3 and section 4.

2. Theoretical Analysis

We postulate an isolated film of CO_2 hydrate, which is resting on a seawater/liquid CO_2 interface of infinite extent. The assumptions employed in the present analysis are as follows.

(1) The film is uniform in thickness.

(2) Its periphery is not strongly indented so that we can safely neglect the effect of azimuthal curvature of the periphery on the profile of the external seawater/liquid CO_2 meniscus projected on a vertical plane normal to the periphery.

(3) Both the growth in thickness and that in the horizontal area of the film are slow enough to allow one to assume a static force balance on the film at each instant. Thus, it turns out that only the forces due to gravity and the liquid/liquid interfacial tension act on the film. (No flow-induced force is working.)

* Corresponding author e-mail: m961825@msr.st.keio.ac.jp; fax: +81-45-562-7625 (c/o Y. H. Mori).

S0013-936X(97)00076-X CCC: $15.00
Published on Web 03/04/1998

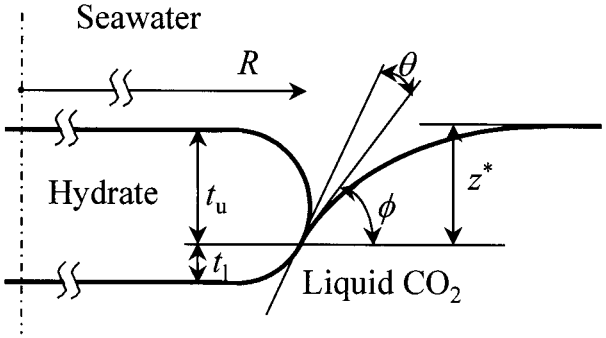

FIGURE 2. Schematic illustration of a hydrate film denser than both liquids and an external liquid/liquid meniscus in mechanical equilibrium.

(4) The film is kept flat and horizontal, thus exhibiting no strain.

(5) Any physical property is constant throughout each of the three phases (seawater, hydrate and liquid CO_2) or over each of the phase boundaries within a vertically narrow space relevant to formulating a force balance in the film.

Assumption 4 may appear to be unreal. The possible effect of elastic deformation of the hydrate film on its stability at the interface is briefly discussed in section 4.

2-1. Force Balance in Mechanical Equilibrium. We first formulate the static force balance for a hydrate film held stationary at the seawater/liquid-CO_2 interface in mechanical equilibrium (see Figure 2). The forces vertically acting on the film are the weight of the film itself, the buoyancy exerted on the film by the surrounding liquids, and the vertical component of the interfacial tension force acting at the three-phase contact line along the periphery of the film. The balance of these forces along the vertical axis is given as

$$\pi R^2\{\rho_h t g + [p_i - \rho_w(z^* - t_u)g] - [p_i - \rho_c(z^* + t_l)g]\} - 2\pi R\zeta\gamma_{cw}\sin\phi = 0$$

or on a unit area basis

$$\rho_h t g + \rho_w(z^* - t_u)g - \rho_c(z^* + t_l)g - \frac{2\zeta\gamma_{cw}}{R}\sin\phi = 0 \qquad (1)$$

where R is the radius of a circular area equivalent to the hydrate film; p_i is the pressure at the horizontal seawater/liquid CO_2 interface; γ_{cw} is the seawater/liquid CO_2 interfacial tension; ϕ is the angle of inclination, measured from the horizontal, at which the seawater/liquid CO_2 interface meets the film; ρ_h, ρ_w, and ρ_c are the densities of the hydrate, seawater saturated with CO_2, and liquid CO_2, respectively; g is the acceleration due to gravity; t is the thickness of the hydrate film; t_u and t_l are the thicknesses of the upper and lower portions, respectively, of the hydrate film, divided by the datum plane including the three-phase contact line; z^* is the height of the meniscus above the datum plane; and ζ is the ratio of the peripheral length of the hydrate film to that of the area-equivalent circle (≥ 1). (It should be noted that throughout this paper, the phrase "seawater saturated with CO_2" or "CO_2-saturated seawater" is used to express a *seawater-rich liquid solution in equilibrium with CO_2 hydrate*. ρ_w is defined as the density of such a solution. See Appendix I.)

Listed below are some remarks on the nature of ϕ and z^*. ϕ is not uniquely determined by the relative wettabilities of the hydrate-crystal surface with the two liquids, which may be evaluated in terms of the seawater-side contact angle (θ), but can vary with the shape, projected on a vertical plane, of the periphery of the film and also with the net gravitational force (i.e., the sum of the first three terms on the left-hand side of eq 1). This is because there is a freedom in microscale positioning of the three-phase contact line at the periphery of the film. A change in the net gravitational force would cause a microscopic displacement of the contact line such that ϕ is so readjusted as to make the interfacial tension force maintain a balance with the net gravitational force.

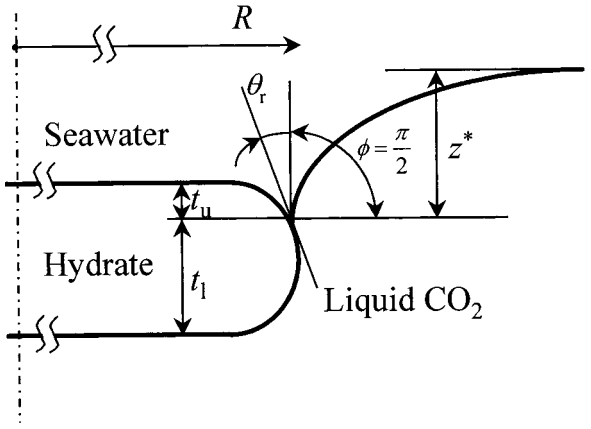

FIGURE 3. Hydrate film denser than both liquids critically suspended at the liquid/liquid interface.

z^* is a function of $\rho_c - \rho_w$, g, γ_{cw}, R, and ϕ, and it can be evaluated by numerically solving the Young−Laplace equation (*3*). Only for the extreme case that $R \to \infty$, z^* has an analytic solution (*4*), which we will utilize later.

As long as eq 1 is satisfied with ϕ appropriately adjusted, the hydrate film should be stably suspended at the interface.

2-2. Critical Conditions for Hydrate Films at the Interface. On the basis of the general force balance given in the previous section, the critical conditions for hydrate films to be suspended at the seawater/liquid CO_2 interface are then considered. For the sake of clarity of further analysis, we distinguish the three possible situations: (i) $\rho_w < \rho_c < \rho_h$, (ii) $\rho_w \leq \rho_h \leq \rho_c$, and (iii) $\rho_h < \rho_w < \rho_c$.

In situation i, the hydrate may sink into the CO_2 pond. Situation ii ensures the absolute stability of the hydrate films at the interface. In situation iii, hydrate films may be released and ascend in the sea. Thus, the critical conditions in situations i and iii are considered in order.

2-2-1. Critical Condition for Hydrate Films Denser Than Liquids ($\rho_w < \rho_c < \rho_h$). As the critical condition beyond which a hydrate film is to sink into the liquid CO_2 phase is approached (e.g., as the result of radial growth of the film), the three-phase contact line at the periphery of the film should recede upward on a microscopic scale till ϕ is increased to $\pi/2$ (when $\theta_r \leq \pi/2$) or $\pi - \theta_r$ (when $\theta_r > \pi/2$), thereby maximizing the force with which the film is attached to the interface (Figure 3). θ_r is the receding seawater-side contact angle, i.e., the possible minimum of θ, and is presumably quite small. This is because any clathrate hydrate is an ice-like crystalline compound primarily composed of hydrogen-bonded water molecules, and hence it is reasonable to assume that the hydrate is more wettable with water than with the hydrate former (CO_2 in the present subject). Thus, we can assume that $\phi \to \pi/2$ at the critical condition, and hence eq 1 reduces to

$$Ig - \frac{2\zeta\gamma_{cw}}{R} = 0 \qquad (2)$$

where

$$I = (\rho_h - \rho_c)t - (\rho_c - \rho_w)(z^* - t_u) \qquad (3)$$

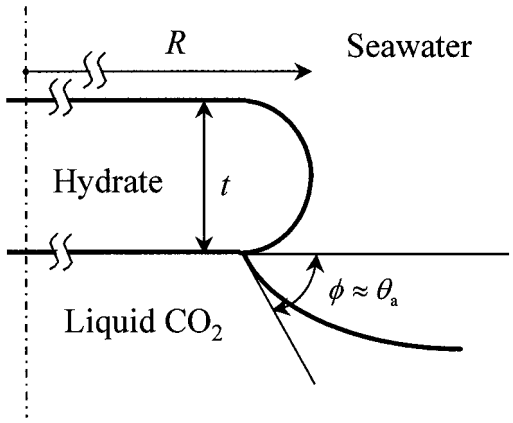

FIGURE 4. Hydrate film less dense than both liquids critically suspended at the liquid/liquid interface.

In the limit as $R \to \infty$, z^* has an analytic solution that is given by

$$z^* = \sqrt{\frac{2}{c}(1 - \cos\phi)} \tag{4}$$

where $c \equiv (\rho_c - \rho_w)g/\gamma_{cw}$ (*4*). In practice, the above solution for $R \to \infty$ overestimates z^* for finite R by no more than 3% on the condition that $Rc^{1/2} > 14$, which corresponds to $R >$ 30 cm at the depth of 4000 m.

Substituting eq 4, in which ϕ is assumed to be $\pi/2$, into eq 3 and distinguishing the resultant quantity I by I_∞, we obtain

$$I_\infty = (\rho_h - \rho_c)t(1 - \mathrm{Fs}_s) \tag{5}$$

where Fs_s is a dimensionless modulus defined as

$$\mathrm{Fs}_s = \frac{\rho_c - \rho_w}{\rho_h - \rho_c}\frac{\sqrt{2/c} - t_u}{t} \tag{6}$$

If $\mathrm{Fs}_s > 1$ and therefore I_∞ is negative, eq 2 has no solution for R. This means that hydrate films can be safely suspended at the seawater/liquid CO_2 interface even for $R \to \infty$. If $\mathrm{Fs}_s < 1$ and therefore I_∞ is positive, there may exist a critical radius ($R_{cr,s}$) beyond which hydrate films are no longer suspended at the interface. In general, $R_{cr,s}$ can be determined by numerically solving eq 2 together with the Young–Laplace equation for evaluating z^* for finite R. If $R_{cr,s}$ is large enough to permit the use of eq 4, a closed form expression for $R_{cr,s}$ can be readily derived, combining eqs 2–4 and setting ϕ at $\pi/2$, as

$$R_{cr,s} = \frac{2\zeta\gamma_{cw}}{(\rho_h - \rho_c)g}\frac{1}{1 - \mathrm{Fs}_s} \tag{7}$$

For hydrate films thinner than ~1 mm, $\sqrt{2/c} \gg t_u$ and hence Fs_s is well approximated by

$$\mathrm{Fs}_s = \frac{\rho_c - \rho_w}{\rho_h - \rho_c}\frac{\sqrt{2/c}}{t} = \frac{\sqrt{2(\rho_c - \rho_w)\gamma_{cw}/g}}{(\rho_h - \rho_c)t} \tag{8}$$

We call Fs_s given by eq 6 or 8 *the film suspension number for possible film sinking* hereafter.

2-2-2. Critical Condition for Hydrate Films Less Dense Than Liquids ($\rho_h < \rho_w < \rho_c$). Here we assume a hydrate film critically suspended at the seawater/liquid CO_2 interface with the geometry illustrated in Figure 4. It is assumed that the contact line has advanced almost to the rear side of the hydrate film so that ϕ (the angle of decline of the external meniscus hung from the contact line) is nearly equal to θ_a (the advancing seawater-side contact angle on the hydrate surface), which is presumably much smaller than $\pi/2$. (ϕ may be slightly different from θ_a, depending on the geometry of the hydrate-film periphery.)

A force balance consideration essentially analogous to that given in the preceding subsection yields Fs_f (the *film suspension number for possible film floating*) and $R_{cr,f}$ (the critical film radius for floating) as

$$\mathrm{Fs}_f = \frac{\rho_c - \rho_w}{\rho_w - \rho_h}\frac{\sqrt{2(1 - \cos\phi)/c}}{t} = \frac{\sqrt{2(\rho_c - \rho_w)(\gamma_{cw}/g)(1 - \cos\phi)}}{(\rho_w - \rho_h)t} \tag{9}$$

$$R_{cr,f} = \frac{2\zeta\gamma_{cw}\sin\phi}{(\rho_w - \rho_h)t}\frac{1}{1 - \mathrm{Fs}_f} \tag{10}$$

Whenever $\mathrm{Fs}_f > 1$, even infinitely large hydrate films are held at the interface. If $\mathrm{Fs}_f < 1$, the size of the hydrate films sustainable at the interface is limited to $R \le R_{cr,f}$.

3. Illustrative Examples and Discussion

For predicting the fate of hydrate films formed in a deep-sea environment, we must specify the density ρ_h and the thickness t of the films—the quantities never uniquely determinable. We select two ρ_h values, within the range molecular-structurally possible for alternative use: 1120 and 1049 kg/m^3. The former is consistent with Ohgaki and Hamanaka's observation of coexisting three phases—liquid water, CO_2 hydrate, and liquid CO_2—(*5*), while the latter is consistent with the prediction by Teng et al. (*6*) and with the Raman-spectroscopy-based estimation by Uchida et al. (*7*) (see Appendix III). For over 1000 m beyond the critical depth ($z \approx 3300$ m) at which ρ_c exceeds ρ_w, the former is higher than ρ_c and the latter is lower than ρ_w (Figure 1). (The condition that ρ_c exceeds ρ_w, the density of seawater saturated with CO_2, is indispensable for stable seawater/liquid CO_2 stratification, and hence we limit our predictions to the range $z \ge 3300$ m.)

Laboratory observations of CO_2 hydrate films suggest that they are thin (see, for example, ref 2). However, no one has clarified how thin they are. Furthermore, we have no reliable means to estimate how thick the films may grow at the surface of CO_2 ponds in deep sea with the lapse of time for some tens or hundreds of years. In this context, we suppose a t-range extending to 4 orders—10 μm to 10 mm. The lower limit is the order of the thickness observed with fluorocarbon hydrate films in a small scale laboratory experiment (*8*).

Figure 5 exemplifies the variations in the film suspension numbers (Fs_s and Fs_f) with depth. In evaluating Fs_s by means of eq 6, we have assumed two extreme contact line locations: $t_u = 0$ and $t_u = t$. It is found, however, that the difference in the contact-line location hardly affects Fs_s as long as $t \lesssim$ 1 mm. Figure 5a allows us to conclude that, at any depth slightly exceeding 3300 m, hydrate films as dense as 1120 kg/m^3 can be safely floated at the seawater/liquid CO_2 interface irrespective of their lateral dimensions unless their thicknesses substantially exceed 1 mm. Figure 5b indicates that hydrate films less dense than the liquids may break away from the interface more easily than the denser films as long as ϕ is, as we believe, much smaller than $\pi/2$.

Figure 6 shows the variation in $R_{cr,f}$ for less dense, 1 mm thick hydrate films suspended at the interface at $\phi = 5°$ with a variation in depth within 26 m just below the critical depth, $z = 3606$ m, at which $\mathrm{Fs}_f = 1$. This figure demonstrates that $R_{cr,f}$ safely exceeds 1 m only within several tens of meters

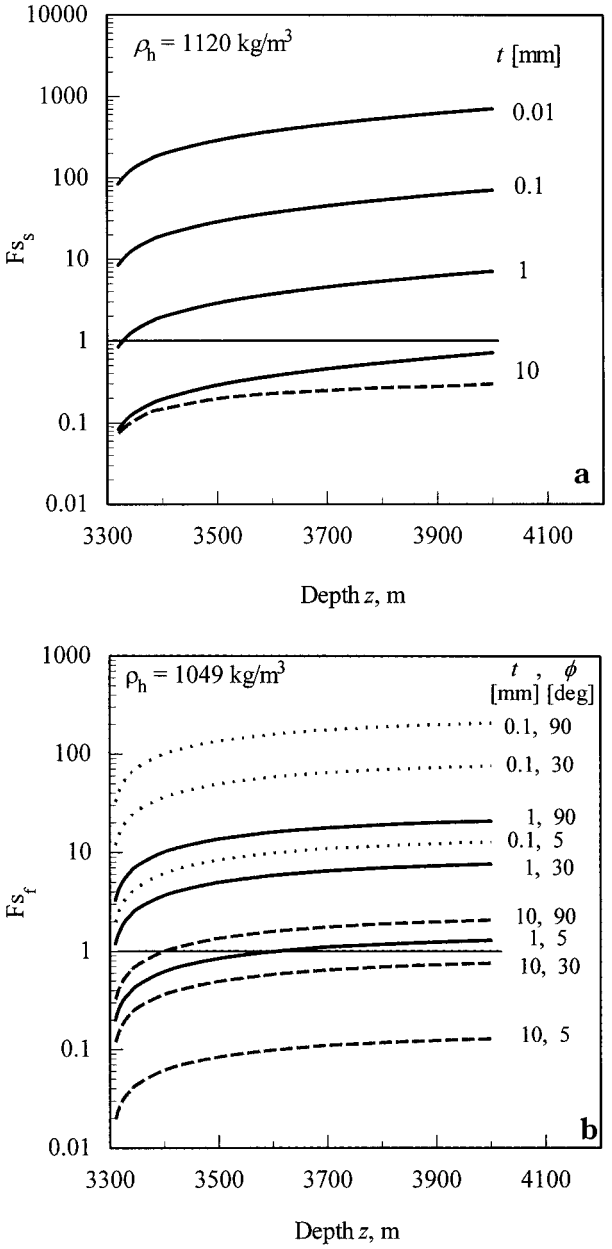

FIGURE 5. Variations in film suspension numbers with the depth from sea level. In panel a, relevant to hydrate films denser than the liquids, solid lines represent predictions for the highest contact-line location, $t_u = 0$, and broken lines represent those for the lowest location, $t_u = t$. In practice, the broken lines are overlapped with the corresponding solid lines except for $t = 10$ mm. In panel b, relevant to hydrate films less dense than the liquids, three different angles are assumed as ϕ, the meniscus slope indicated in Figure 4, for each assumed hydrate-film thickness.

from the critical depth and that it exhibits an enormously sharp increase in close vicinity to the critical depth.

It is interesting to note the intuitively anomalous fact demonstrated in Figure 5b, i.e., the stability of hydrate films represented by Fs_f does not decrease but increases with an increase in z, which yields an increase in the excess of the density of each liquid above ρ_h. This fact is peculiar to any solid body suspended at a deformable fluid/fluid interface. The pressure working on the upper surface of each hydrate film is less than p_i (the pressure at the horizontal interface) by the seawater-side hydrostatic head ($\rho_w(z^* + t)g$), while the pressure on the lower surface is less than p_i by the liquid-CO_2-side hydrostatic head ($\rho_c z^* g$). The excess of the pressure

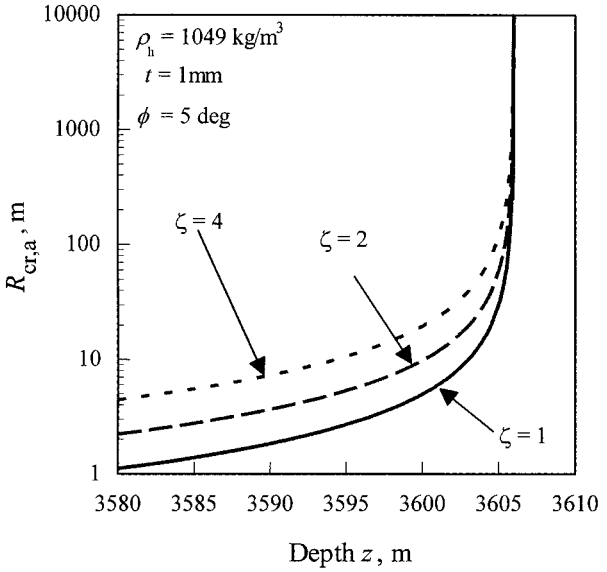

FIGURE 6. Variation in $R_{cr,f}$, the critical radius above which hydrate films float away from the interface, with depth. $R_{cr,f} \to \infty$ at $z = 3606$ m at which $Fs_f = 1$.

on the lower surface above that on the upper surface is necessarily less than $\rho_w tg$, the buoyancy that would work in the bulk of the seawater phase, by the interphase hydrostatic-head difference ($(\rho_c - \rho_w)z^* g$). This quantity increases with an increase in the depth (z) reducing the buoyancy on the hydrate film and thereby even increasing the stability of the film at the interface.

The numerical examples given above may be a warning to such an optimistic view that hydrate films will stay at the CO_2 pond surface, thereby serving as permanent barriers against the CO_2 dissolution into the sea. If the surface of a CO_2 pond is located at a depth of some 3600 m or less, it is possible that hydrate films grown to a ~1 mm thickness break away from the pond surface and then buoy up in the sea rather than sink into the pond, up to the depth at which the seawater and the films are equal in density. During their rise in the sea in which CO_2 is not dissolved to saturation, the hydrate films should dissociate and release CO_2 molecules into the sea. In short, the formation and growth at the pond surface of hydrate films and their successive rise and dissociation in the sea should work as a pond-to-sea CO_2 pumping system. Unless we obtain definite evidence that the CO_2 hydrate less dense than seawater never forms in nature, the possible promotion of the pond-to-sea CO_2 transfer due to the above-mentioned mechanism should be taken into account during the course of feasibility studies of CO_2 disposal into deep oceans.

4. Consideration of Hydrate Film Deformation

In the previous section, we have assumed hydrate films to be rigid planar sheets having an unlimited breaking strength. In practice, hydrate films must be deflected more or less, and they might even be broken due to deflection-dependent stress before they grow enough to detach themselves from the seawater/liquid CO_2 interface. The possibility of such breaking of hydrate films at the interface is examined in this section, assuming the films to be elastic circular sheets ($\zeta = 1$) that are flat only in the absence of any load.

The analytic model we employ is a simple extension of the one dealt with in subsection 2.2.2 (or illustrated in Figure 4): an axisymmetric deflection ($w(r)$) of a uniform hydrate film less dense than the liquids is assumed (see Figure 7). On

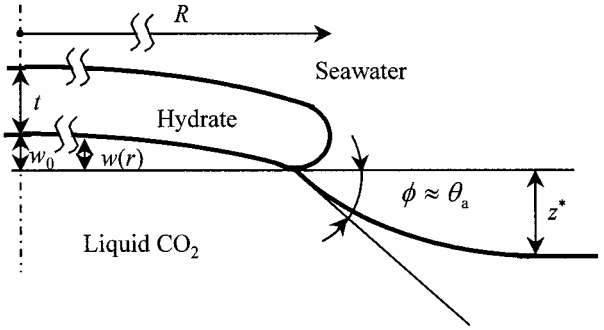

FIGURE 7. Deflected hydrate film suspended at the liquid/liquid interface.

condition that $w(r) \ll R$ over $0 \le r \le R$, the total force balance on the film can be written as

$$\pi R^2 \rho_h t g + 2\pi \int_0^R \{[p_i - \rho_w(z^* + w + t)g] - [p_i - \rho_c(z^* + w)g]\} r\, dr + 2\pi R \gamma_{cw} \sin\phi = 0$$

or

$$\rho_h t g + \frac{2}{R^2}\int_0^R [\rho_c(z^* + w) - \rho_w(z^* + w + t)] g r\, dr + \frac{2\gamma_{cw}}{R}\sin\phi = 0 \quad (11)$$

There is no analytical means to rigorously derive the functional form of $w(r)$ which has to be specified in order to perform the integration in eq 11. Thus, we have conceived a rather crude and approximate solution procedure in which the deflection profile of a uniformly loaded circular plate (*9*) is substituted for $w(r)$ as

$$w(r) = w_0\left[1 - \left(\frac{r}{R}\right)^2\right]^2 \quad (12)$$

where w_0 is the deflection at the center of the plate. Substituting eq 12 together with eq 4 into eq 11, we obtain

$$w_0 = 3\left[\frac{\rho_w - \rho_h}{\rho_c - \rho_w} t - \sqrt{\frac{2}{c}(1 - \cos\phi)} - \frac{2\gamma_{cw}\sin\phi}{(\rho_c - \rho_w) g R}\right] \quad (13)$$

It should be noted that ϕ in eq 13 may deviate from θ_a because the situation of present interest is not necessarily at the critical condition for the hydrate film floating away from the interface. ϕ may adjust itself in the range $0 < \phi \ll \theta_a$ to satisfy the force balance.

To obtain a stress−deflection relation for hydrate films, we rely again on the uniform load approximation. The classical theory of elasticity provides the following expressions for the deflection (w_0) and the stress (σ_0) at the center of a circular, uniformly loaded plate on the condition that $w_0 \lesssim t$ (*9*):

$$w_0 = 0.662R\left(\frac{qR}{Et}\right)^{1/3} \quad (14)$$

$$\sigma_0 = 0.423\left(\frac{Eq^2R^2}{t^2}\right)^{1/3} \quad (15)$$

where q is the distributed load per unit area of the plate and E is Young's modulus of the plate-forming material, i.e., the CO_2 hydrate in the problem we are concerned with. Combining eqs 14 and 15, we have a stress−deflection relation, eliminating q, as

$$\sigma_0 = 0.966E\left(\frac{w_0}{R}\right)^2 \quad (16)$$

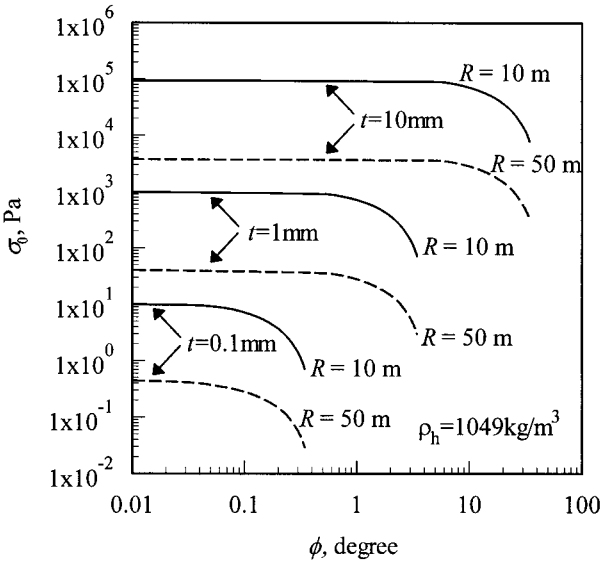

FIGURE 8. Estimated stress at the center of hydrate film at depth of 3700m. The deflection (w_0) decreases with increasing ϕ along each curve. The right-side end of the curve corresponds to the condition $w_0 = t$, beyond which eqs 14−16 may be inaccurate.

The magnitudes of σ_0 in hydrate films are estimated using the following procedure: specifying R, t, and ϕ, eq 13 is used to calculate w_0, which is then substituted into eq 16 to evaluate σ_0. (E in eq 16 is assumed to be 8.4 GPa. See Appendix III.) Figure 8 illustrates how σ_0 varies with R, t, and ϕ at the depth of 3700 m. Unexpectedly, we find that smaller hydrate films ($R = 10$ m) have larger σ_0 values than do the larger hydrate films ($R = 50$ m). This tendency prevails in the regime $t \lesssim w_0 \lesssim R$ in which eqs 13 and 16 are valid, and it never indicates that σ_0 monotonically increases as $R \to 0$.

To judge whether hydrate films can endure the bending stress or not during their growth at the seawater/liquid CO_2 interface, we need to infer if the σ_0 values estimated above are below the ultimate bending strength of the CO_2 hydrate or exceed it. Although we find in the literature some experimental tests of mechanical strength of hydrate films (of unknown thickness) or blocks, none of them provides quantitative information on the bending or tensile strength in terms of stress (see Appendix III). We can only estimate that the limit of σ_0 sustainable by hydrate films is not higher than, though not deviating far from, the tensile strength of single water-ice crystals—0.05−0.5 MPa (*10*). In view of this tentative criterion, it may be said that hydrate films are likely to be broken before growing to some 10 mm in thickness at the seawater/liquid CO_2 interface.

Appendix I. How Liquid CO_2 Is Deposited on Sea Floors—Ponds or Piles of Hydrate-Covered Drops?

There is a conventional notion that liquid CO_2 piped to a basin on the sea floor deeper than 3000 m forms a pond (or a lake) having a planar surface—the seawater/liquid CO_2 interface (*2*). Currently, there are some researchers that have some doubt about this notion. In a recent paper of Teng (*11*), for example, he asserted that liquid CO_2 injected into the deep ocean will be deposited in the form of a pile of hydrate-covered drops instead of a pond because hydrate films covering drops will prevent the drops from mutually

TABLE 1. Mass Density of CO_2 Hydrate: List of Its Values Reported in the Literature

ref	ρ_h (kg/m^3)	
Ohgaki and Hamanaka (*5*)	1110−1126	observed
Teng *et al.* (*6*)	1049 (av) (max 1134; min 1007)	crystallographic prediction
Uchida *et al.* (*7*)	1040−1060	Raman spectroscopy
Yamane and Aya (*16*)	1109	calculated from measured dissociation heat
Unruh and Katz (*21*)	less dense than water	observed
Takenouchi and Kennedy (*22*)	1150	calculated from measured dissociation heat

coalescing into a continuous phase. This droplet-pile hypothesis is solely based on visual observations in small-scale laboratory experiments (*12, 13*), in which liquid CO_2 was dripped through a fine tubular nozzle into freshwater or seawater, resulting in a piling of hydrate-covered CO_2 drops up to the height of several centimeters. It should be reminded, however, that in case of actual CO_2 disposal, liquid CO_2 will be discharged from a vertical pipe, presumably several tens of centimeters in diameter, into a basin to be deposited to several tens of meters (or more) in thickness, laterally extending to several hundred meters (at least). We assume that if the hydrate-covered CO_2 drops are piled to a significant height, those in the lower layers will be readily crushed and form a continuous liquid CO_2 phase. It is our belief that a pond will be formed and that its surface will be flat except for a relatively small area, beneath the opening of the vertical pipe, over which hydrate-covered CO_2 drops may be piled. If the opening of the pipe is located below the level of the pond surface as illustrated in Yamane and Aya (*14*), drops will no longer be piled on the surface.

Appendix II. Evaluation of Physical Properties of Seawater and Liquid CO_2

Curve-fitting correlations for the temperature (T) and the seawater density (ρ_{w0}), have been prepared as functions of the depth from sea level (z), by applying regression analysis procedures to the $T - z$ and $\rho_{w0} - z$ data compiled by Liro et al. (*15*), plus one $T - z$ data referred to by Hirai et al. (*16*). They are

$$\frac{T}{[\mathrm{K}]} = \frac{3946}{\dfrac{z}{[\mathrm{m}]} + 112} + 273.6 \qquad \left(100 \lesssim \frac{z}{[\mathrm{m}]} \lesssim 5200\right) \tag{A-1}$$

$$\frac{\rho_{w0}}{[\mathrm{kg/m^3}]} = 5.89 \times 10^{-11}\left(\frac{z}{[\mathrm{m}]}\right)^3 - 5.38 \times 10^{-7}\left(\frac{z}{[\mathrm{m}]}\right)^2 + 6.10 \times 10^{-3}\left(\frac{z}{[\mathrm{m}]}\right) + 1026.3 \qquad \left(100 \lesssim \frac{z}{[\mathrm{m}]} \lesssim 5200\right) \tag{A-2}$$

The pressure (p) as a function of z is obtained by integrating $\rho_{w0}g$ along the z axis and adding the atmospheric pressure value:

$$\frac{p}{[\mathrm{Pa}]} = 1.44 \times 10^{-10}\left(\frac{z}{[\mathrm{m}]}\right)^4 - 1.75 \times 10^{-6}\left(\frac{z}{[\mathrm{m}]}\right)^3 + 2.99 \times 10^{-2}\left(\frac{z}{[\mathrm{m}]}\right)^2 + 1.01 \times 10^{4}\left(\frac{z}{[\mathrm{m}]}\right) + 1.01 \times 10^{5} \tag{A-3}$$

The interfacial tension (γ_{cw}) is estimated to be about 24 mN/m at depths of 3300−4000m using Donahue and Bartell's correlation (*17*) in which the CO_2-in-water and water-in-CO_2 solubility values (*14, 18, 19*) are substituted.

The density of liquid CO_2 (ρ_c) at each depth (z) is evaluated using eqs A-1 and A-3 (for the $z \rightarrow T$ and $z \rightarrow p$ conversions, respectively) and then PROPATH (*20*) for the computation of $\rho_c(p,T)$.

The seawater near the interface with a liquid CO_2 phase should be nearly saturated with CO_2, and hence its density is presumed to be higher than ρ_{w0}, the ordinary seawater density, at the same temperature and pressure. It would be reasonable to assume that, in the presence of a hydrate film at the interface, the composition of the seawater in the vicinity of the film approximates that of the seawater-rich liquid solution thermodynamically in equilibrium with the CO_2 hydrate. The density of such CO_2-saturated seawater (ρ_w) is estimated as follows. Some experimental observations of Shindo et al. (*2*) suggest that the CO_2-saturated water and liquid CO_2 both coexisting with CO_2 hydrate are nearly equal in density at $p = 35$ MPa and $T = 3$ °C. On the other hand, PROPATH predicts that $\rho_c \approx 1059$ kg/m^3 under that thermodynamic condition. Thus, we can presume that $\rho_w(z)$ shifts from $\rho_{w0}(z)$ so that the $\rho_w(z)$ and $\rho_c(z)$ curves cross each other at the density level of 1059 kg/m^3. Because of the lack of any other information about ρ_w, we simply assume a parallel shift of $\rho_w(z)$ from $\rho_{w0}(z)$ as

$$\frac{\rho_w}{[\mathrm{kg/m^3}]} = \frac{\rho_{w0}}{[\mathrm{kg/m^3}]} + 17 \tag{A-4}$$

Equation A-4 combined with eq A-2 predicts that the condition $\rho_c > \rho_w$ is satisfied at depths beyond 3300 m (see Figure 1).

Appendix III. Physical Properties of CO_2 Hydrate

III-1. Mass Density of CO_2 Hydrate. Table 1 summarizes the experimental data and theoretical predictions of the density of the CO_2 hydrate (ρ_h) found in the literature. Some qualitative observations indicating the possible range of ρ_h are also included in the table. Here we note a considerable scatter in the ρ_h values reported so far. Brief comments on the contents of the table are given below for the readers' reference.

Unruh and Katz (*21*) observed dissociating CO_2 hydrate flakes floating at a liquid water/gaseous CO_2 interface; hence, they claimed that the CO_2 hydrate is less dense than liquid water. Their observation was criticized later by Takenouchi and Kennedy (*22*), who suspected that the apparent flotation of hydrate flakes in Unruh and Katz's observation was ascribed to the generation of tiny CO_2 gas bubbles within the hydrate flakes. The generation of such CO_2 gas bubbles was certainly possible in Unruh and Katz's experiments; however, we cannot confirm the actual generation of such bubbles in those experiments. Thus, we have included Unruh and Katz's statement about ρ_h in Table 1.

Contrary to Unruh and Katz's observation discussed above, the recent work of Ohgaki and Hamanaka (*5*) suggests a rather high ρ_h value. Based on their observations of the three phases—liquid water, liquid CO_2, and CO_2

TABLE 2. Mass Density of CO_2 Hydrate: Prediction of Its Dependency on the Fractional Occupancies of Cavities

occupancy x_s (5^{12} cavities) (%)	occupancy x_l ($5^{12}6^2$ cavities) (%)	hydrate density ρ_h (kg/m^3)	hydration number n
95	100	1130	5.82
75	100	1113	6.13
50	100	1092	6.57
30	100	1075	6.97
20	100	1067	7.19
10	100	1058	7.42
0	100	1049	7.67
30	95	1063	7.30
20	95	1054	7.54
10	95	1046	7.80

hydrate—coexisting in a high-pressure cell, Ohgaki and Hamanaka reported that $\rho_h > \rho_c$ at $T = 288.10$ K and $p = 72.77$ MPa but $\rho_h < \rho_c$ at $T = 288.59$ K and $p = 82.20$ MPa; from this information, we can readily deduce the possible range for ρ_h as indicated in Table 1.

The value of ρ_h can be readily estimated based on a crystallographic theory, once we are informed of the occupancies, with CO_2 molecules, of six larger tetrakaidecahedron ($5^{12}6^2$) cavities and two smaller pentagonal dodecahedron (5^{12}) cavities, respectively, in each unit cell of the hydrate, or alternatively of the hydration number n (the number of water molecules per CO_2 molecule in the hydrate). The occupancy of the 5^{12} cavities with CO_2 molecules is a point of current controversy; the results of a recent Raman spectroscopic study of Sum et al. (*23*) indicate no occupancy of the smaller cavities with CO_2 molecules, while an NMR study of Udachin et al. (*24*) indicates some occupancy. Based on their Raman spectroscopic study, Uchida et al. (*7*) determined that $n \approx 7.24-7.68$, from which they estimated the possible range of ρ_h indicated in Table 1.

The following is a quantitative demonstration of the relation of ρ_h to the cavity occupancies or the hydration number. On the basis of a well-established crystallographic theory, ρ_h can be estimated with a reasonable accuracy using the equation shown below, counting the contributions of H_2O and CO_2 molecules to the total mass of a unit cell of the structure I hydrate:

$$\rho_h = \frac{18.015 \times 46 + 2 \times 44.010 \times x_s + 6 \times 44.010 \times x_l}{Aa^3} = \frac{46 \times (18.015 + 44.010/n)}{Aa^3} \quad \text{(A-5)}$$

where A is the Avogadro number, a is the cubic cell parameter for the structure I hydrate, which is assumed to be 12 Å (*25*), and x_s and x_l are the fractional occupancies of smaller and larger cavities, respectively, with CO_2 molecules. Table 2 lists the ρ_h values deduced based on different assumptions of x_s and x_l (or n). The estimations of ρ_h given in Table 2 indicate that, unless the occupancy of the smaller cavities exceeds some 10−20%, the hydrate is less dense than both the liquid CO_2 and CO_2-saturated seawater at depths greater than ~3300 m.

Having reviewed the data sources for the density or the cavity occupancies for the CO_2 hydrate, we find no conclusive evidence that the CO_2 hydrate is denser or less dense than seawater under pressures corresponding to the depths exceeding ~3300 m. The cavity occupancies (particularly the occupancy of the smaller cavities) and hence the density of the CO_2 hydrate may not be unique under a given pressure and temperature, but they may vary, for example, with the lapse of time after its formation and/or the convective or diffusive transfer of CO_2 to or from the surrounding seawater phase. It is our opinion that we should not give an impatient conclusion to the evaluation of the CO_2 hydrate density before the above-mentioned issue is clarified.

III-2. Mechanical Properties of Hydrates. In recent years, some research groups attempted to measure the mechanical strength of polycrystalline hydrate samples. Aya et al. (*26*) reported the tensile strength of a hydrate film formed at a planar liquid CO_2/liquid water interface to be ~1.3 N/m. (In ref 26a, the strength is given as 0.13 N/m. This is a typographical error of 1 order. The strength is correctly written in the Japanese version of the above report, ref 26b.) Uchida and Kawabata (*27*) evaluated the tensile strength of shell-shaped hydrate films each enclosing a water drop in a liquid CO_2 medium to be 6−17 N/m. Note that these strength values are given not in terms of "stress" but in terms of the product of the stress and the film thickness; this is because the thicknesses of the sample hydrate films used in those strength measurements were unknown. Recently, Stern et al. (*28*) and Ebinuma (*29*) reported the strength, expressed in terms of stress, of methane and tetrahydrofuran hydrates, respectively. However, these strength values were derived from compression tests, instead of bending or tensile tests, of cylindrical hydrate blocks. We find in the existing literature no experimental data on the bending or tensile strength of any kind of clathrate hydrates expressed in terms of stress.

No direct measurement of Young's modulus (E) of any clathrate hydrate has been reported. What we can refer to at present about Young's modulus is only its estimation from the sound speed through a structure I hydrate. The estimation gives $E = 8.4$ GPa (*30*).

Glossary

a	cubic cell parameter for structure I hydrate (m)
A	Avogadro number (molecules/kmol)
c	capillary constant defined in eq 4 as $(\rho_c - \rho_w)g/\gamma_{cw}$ (1/m^2)
E	Young's modulus of hydrate (Pa)
Fs_f	film suspension number for possible film floating defined in eq 10 (−)
Fs_s	film suspension number for possible film sinking defined in eq 6 or 8 (−)
g	acceleration due to gravity (m/s^2)
I	quantity defined in eq 3 (kg/m)
I_∞	quantity defined in eq 5 (kg/m)
n	hydration number (−)
p	pressure (Pa)
p_i	pressure at the horizontal seawater/liquid CO_2 interface (Pa)
q	distributed load per unit area of hydrate (Pa)
R	radius of a circular area equivalent to hydrate film (m)
$R_{cr,f}$	critical value of R beyond which a hydrate film floats into the liquid CO_2 phase (m)
$R_{cr,s}$	critical value of R beyond which a hydrate film sinks into the liquid CO_2 phase (m)
t	thickness of hydrate film (m)
t_l	thickness of the lower portion of the hydrate film below the datum plane including the seawater/liquid CO_2/hydrate contact line (m)
t_u	thickness of the upper portion of hydrate film above the datum plane including the seawater/liquid CO_2/hydrate contact line (m)
T	temperature (K)

w local deflection of hydrate film (m)

w_0 deflection of the center of hydrate film (m)

x_l fractional occupancy of $5^{12}6^2$ cavities with CO_2 molecules (−)

x_s fractional occupancy of 5^{12} cavities with CO_2 molecules (−)

z depth from sea level (m)

z^* height of the external meniscus measured from the datum plane including the seawater/liquid CO_2/hydrate contact line (m)

Greek Letters

γ_{cw} seawater/liquid CO_2 interfacial tension (N/m)

ζ ratio of the peripheral length of hydrate film to that of area-equivalent circle (−)

θ seawater-side contact angle on hydrate film (deg)

θ_a advancing seawater-side contact angle on hydrate film (deg)

θ_r receding seawater-side contact angle on hydrate film (deg)

ρ_c density of liquid CO_2 (kg/m^3)

ρ_h density of hydrate (kg/m^3)

ρ_w density of seawater saturated with CO_2 (kg/m^3)

ρ_{w0} density of ordinary seawater (kg/m^3)

σ_0 stress at the center of hydrate film (Pa)

ϕ angle of inclination, measured from the horizontal, at which seawater/liquid CO_2 interface meets hydrate film (deg)

Literature Cited

(1) Ribeiro, J.; Henry, B. *Carbon Dioxide Disposal and Storage Technologies*, Institute for Prospective Technological Studies, Joint Research Centre, European Commission: 1995.

(2) Shindo, Y.; Fujioka, Y.; Ozaki, M.; Yanagisawa, Y.; Hakuta, T.; Komiyama, H. In *Direct Ocean Disposal of Carbon Dioxide*; Handa, N., Ohsumi, T., Eds.; Terrapub: Tokyo, 1995; pp 217−231.

(3) Hartland, S.; Hartley, W. R. *Axisymmetric Fluid−Liquid Interfaces*; Elsevier: Amsterdam, 1976; Chapter 4.

(4) Princen, H. M. In *Surface and Colloid Science*, Vol. 2; Matijevic, E., Ed.; Wiley: New York, 1969; pp 1−84.

(5) Ohgaki, K.; Hamanaka, T. *Kagaku Kogaku Ronbunshu* **1995**, *21*, 800.

(6) Teng, H.; Yamasaki, A.; Shindo Y. *Chem. Eng. Sci.* **1996**, *51*, 4979.

(7) Uchida, T.; Takagi, A.; Kawabata, J.; Mae, S.; Hondo, T. *Energy Convers. Manage.* **1995**, *36*, 547.

(8) Sugaya, M.; Mori, Y. H. *Chem. Eng. Sci.* **1995**, *51*, 3505.

(9) Timoshenko, S. P.; Woinowsky-Kreiger S. *Theory of Plates and Shells*, 2nd ed.; McGraw-Hill: Tokyo, 1959.

(10) Fletcher, N. H. *The Chemical Physics of Ice*; Cambridge University Press: London, 1970.

(11) Teng, H. *Int. J. Chem. Kinet.* **1996**, *28*, 935.

(12) Hirai, S.; Okazaki, K.; Araki, N.; Yoshimoto, K.; Ito, H.; Hijikata, K. *Energy Convers. Manage.* **1995**, *36*, 471.

(13) Nishikawa, N.; Ishibashi, M.; Ohta, H.; Akutsu, N.; Tajika, M.; Sugitani, T.; Hiraoka, H.; Kimuro, H.; Shiota, T. *Energy Convers. Manage.* **1995**, *36*, 489.

(14) Yamane, K.; Aya, I. *Proceedings of the International Conference on Technologies for Marine Environment Preservation*; Society of Naval Architects of Japan: Tokyo, 1995; Vol. 2, pp 911−917.

(15) Liro, C. R.; Adams, E. E.; Herzog, H. J. *Modeling the Release of CO_2 in the Deep Ocean*; MIT-EL 91-002; MIT: Cambridge, MA, 1991.

(16) Hirai, S.; Okazaki, K.; Tabe, Y.; Hijikata, K.; Mori, Y. *Energy* **1997**, *22*, 363.

(17) Donahue, D. J.; Bartell, F. E. *J. Phys. Chem.* **1952**, *56*, 480.

(18) Dodds, W. S.; Stutzman, L. F.; Sollami, B. J. *Ind. Eng. Chem., Chem. Eng. Data Ser.* **1956**, *1*, 92.

(19) Song, K. Y.; Kobayashi, R. *SPE Form. Eval.* **1987**, *2*, 500.

(20) *PROPATH−a Program Package for Thermophysical Properties of Fluids*, Version 7.1; Corona Publishing: Tokyo, 1990.

(21) Unruh, C. H.; Katz, D. L. *Petroleum Transactions*; AIME: New York, April 1949; pp 83−86.

(22) Takenouchi, S.; Kennedy, G. C. *J. Geol.* **1965**, *73*, 383.

(23) Sum A. K.; Burruss R. C.; Sloan, E. D., Jr. *J. Phys. Chem. B* **1997**, *101*, 7371.

(24) Udachin, K. A.; Enright, G. D.; Ratcliffe, C. I.; Ripmeester, J. A. *Prepr. Pap., Am. Chem. Soc., Div. Fuel Chem.* **1997**, *42* (2), 467.

(25) Sloan, E. D., Jr. *Clathrate Hydrates of Natural Gases*; Dekker: New York, 1990; Chapter 2.

(26) (a) Aya, I.; Yamane, K.; Yamada, N. In *Fundamentals of Phase Change: Freezing, Melting, and Sublimation−1992* (HTD-Vol. 215); Kroegaer, P. E., Bayazitoglu, Y., Eds.; American Society of Mechanical Engineers: New York, 1992; pp 17−22. (b) Aya, I.; Yamane, K.; Yamada, N. *Trans. Jpn. Soc. Mech. Eng.* **1993**, *59B*, 1210.

(27) Uchida, T.; Kawabata, J. *Energy* **1997**, *2/3*, 357.

(28) Stern, L. A.; Kirby, S. H.; Durham, W. B. *Science* **1996**, *273*, 1843.

(29) Ebinuma, T. *Proceedings of the International Workshop on Gas Hydrate Studies*; Geological Survey of Japan: Tsukuba, Japan, 1997; pp 159−163.

(30) Davidson, D. W. In *Natural Gas Hydrates*: *Properties, Occurrence and Recovery*; *Gas Hydrates as Clathrate Ices*; Cox, J. L., Ed.; Butterworth: Boston, 1983; p 13.

Received for review January 29, 1997. Revised manuscript received January 12, 1998. Accepted January 26, 1998.

ES9700764